










## ORIGINAL ARTICLE

# Identification and characterization of *Cercospora beticola* necrosis-inducing effector CbNip1

Malaika K. Ebert <sup>1,2,3</sup> | Lorena I. Rangel <sup>1</sup> | Rebecca E. Spanner <sup>1,2</sup> |  
 Demetris Taliadoros<sup>4,5</sup> | Xiaoyun Wang<sup>1</sup> | Timothy L. Friesen <sup>1,2</sup> |  
 Ronnie de Jonge <sup>6,7,8</sup> | Jonathan D. Neubauer<sup>1</sup> | Gary A. Secor <sup>2</sup> |  
 Bart P. H. J. Thomma <sup>3,9</sup> | Eva H. Stukenbrock <sup>4,5</sup> | Melvin D. Bolton <sup>1,2</sup>

<sup>1</sup>Edward T. Schafer Agricultural Research Center, USDA Agricultural Research Service, Fargo, North Dakota, USA

<sup>2</sup>Department of Plant Pathology, North Dakota State University, Fargo, North Dakota, USA

<sup>3</sup>Laboratory of Phytopathology, Wageningen University, Wageningen, Netherlands

<sup>4</sup>Environmental Genomics Group, Max Planck Institute for Evolutionary Biology, Plön, Germany

<sup>5</sup>Christian-Albrechts University of Kiel, Kiel, Germany

<sup>6</sup>Plant-Microbe Interactions, Department of Biology, Utrecht University, Utrecht, Netherlands

<sup>7</sup>Department of Plant Systems Biology, VIB, Ghent, Belgium

<sup>8</sup>Department of Plant Biotechnology and Bioinformatics, Ghent University, Ghent, Belgium

<sup>9</sup>University of Cologne, Institute for Plant Sciences, Cluster of Excellence on Plant Sciences (CEPLAS), Cologne, Germany

**Correspondence**

Melvin D. Bolton, Edward T. Schafer Agricultural Research Center, USDA Agricultural Research Service, Fargo, ND, USA.  
 Email: melvin.bolton@usda.gov

**Present address**

Malaika K. Ebert, Department of Plant Biology, Michigan State University, East Lansing, Michigan, USA  
 Xiaoyun Wang, Institute of Biotechnology, Cornell University, Ithaca, New York, USA

**Abstract**

*Cercospora beticola* is a hemibiotrophic fungus that causes cercospora leaf spot disease of sugar beet (*Beta vulgaris*). After an initial symptomless biotrophic phase of colonization, necrotic lesions appear on host leaves as the fungus switches to a necrotrophic lifestyle. The phytotoxic secondary metabolite cercosporin has been shown to facilitate fungal virulence for several *Cercospora* spp. However, because cercosporin production and subsequent cercosporin-initiated formation of reactive oxygen species is light-dependent, cell death evocation by this toxin is only fully ensured during a period of light. Here, we report the discovery of the effector protein CbNip1 secreted by *C. beticola* that causes enhanced necrosis in the absence of light and, therefore, may complement light-dependent necrosis formation by cercosporin. Infiltration of CbNip1 protein into sugar beet leaves revealed that darkness is essential for full CbNip1-triggered necrosis, as light exposure delayed CbNip1-triggered host cell death. Gene expression analysis during host infection shows that *CbNip1* expression is correlated with symptom development in planta. Targeted gene replacement of *CbNip1* leads to a significant reduction in virulence, indicating the importance of CbNip1 during colonization. Analysis of 89 *C. beticola* genomes revealed that *CbNip1* resides in a region that recently underwent a selective sweep, suggesting selection pressure exists to maintain a beneficial variant of the gene. Taken together, CbNip1 is a crucial effector during the *C. beticola*-sugar beet disease process.

**KEYWORDS**

*Cercospora beticola*, necrosis-inducing effector, virulence factor

Malaika K. Ebert and Lorena I. Rangel contributed equally to this work.

This is an open access article under the terms of the Creative Commons Attribution-NonCommercial-NoDerivs License, which permits use and distribution in any medium, provided the original work is properly cited, the use is non-commercial and no modifications or adaptations are made.

© 2020 This article is a U.S. Government work and is in the public domain in the USA. *Molecular Plant Pathology* published by John Wiley & Sons Ltd

## 1 | INTRODUCTION

Cercospora leaf spot (CLS) disease is considered one of the most destructive foliar diseases of sugar beet worldwide (Rangel et al., 2020). The causal agent of CLS is the hemibiotrophic fungus *Cercospora beticola*, which belongs to the Dothideomycete class (Bolton et al., 2012). In the field, *C. beticola* overwinters as stromata, which serves as the primary inoculum in the following growing season (Khan & Khan, 2010; Rangel et al., 2020; Solel & Minz, 1971). Once infection is established, airborne conidia can be quickly dispersed throughout the field by wind, rain, and insect transfer (Khan & Khan, 2010; Rangel et al., 2020). On landing on a sugar beet leaf, spores germinate and grow towards stomata, where they form appressoria (Feindt et al., 1981; Rangel et al., 2020; Rathaiah, 1977). These hyphal structures enable the fungus to penetrate and enter the apoplast (Steinkamp et al., 1979). Once inside the host, *C. beticola* grows intercellularly and colonizes the mesophyll for up to 10 days (Rangel et al., 2020). During these early stages of infection, *C. beticola* lives a biotrophic lifestyle. However, unknown conditions trigger hemibiotrophic fungi to switch from a biotrophic to a necrotrophic lifestyle in which host cell death occurs to complete their life cycle (Horbach et al., 2011; Steinkamp et al., 1979).

Necrosis-inducing molecules come in many forms and with various modes of actions. For example, necrotrophic effectors, also known as proteinaceous host-selective toxins, depend on the presence of a corresponding target encoded by a susceptibility gene in their host to elicit host cell death (Faris et al., 2010; Friesen et al., 2007, 2008; Shi et al., 2016). This interaction is essentially the classic gene-for-gene interaction (Flor, 1942), but instead of providing resistance to the fungus, host cell death serves the necrotrophic needs of the fungus. Therefore, this interaction is also referred to as an inverse gene-for-gene interaction with host and pathogen traits that coevolve to avoid infection and obtain nutrients, respectively (Friesen et al., 2007). For example, the necrotrophic effector SnTox1 of the wheat pathogen *Parastagonospora nodorum* interacts with Snn1 encoded by a wheat receptor kinase gene, which activates programmed cell death in the host and facilitates a compatible interaction (Liu et al., 2004, 2012; Shi et al., 2016). However, not all necrosis-inducing effectors are dependent on a host receptor to provoke host cell death. A family of Nep1-like proteins (NLPs) has been identified in several oomycetes, fungi, and bacteria that elicit a hypersensitive response-like host necrosis (Gijzen & Nürnberger, 2006; Pemberton & Salmond, 2004). The first family member discovered was Nep1 (necrosis- and ethylene-inducing protein 1), a protein secreted by *Fusarium oxysporum* that was shown to trigger necrosis and ethylene production in *Erythroxylum coca* (coca plant) (Bailey, 1995). Besides high sequence homology, NLPs share a common necrosis-inducing *Phytophthora* protein (NPP1) domain (Fellbrich et al., 2002). Motteram et al. (2009) reported an NPP1 domain-carrying phytotoxic effector called MgNlp that is expressed during infection of the hemibiotrophic pathogen *Zymoseptoria tritici*, the causal agent of septoria tritici blotch on wheat. Furthermore, necrosis-inducing activity was described as selective because MgNlp induced

cell death in *Arabidopsis* and tobacco but not in wheat. Interestingly, targeted gene replacement of MgNlp did not affect fungal virulence in inoculation studies of susceptible wheat lines (Motteram et al., 2009). Additionally, analysis of *Z. tritici* culture filtrates led to the discovery of two light-dependent phytotoxic proteins, ZtNip1 and ZtNip2, whose activities resemble those of host-specific toxins (Ben M'Barek et al., 2015). While ZtNip1 displays homology to the *Cladosporium fulvum* effector protein Ecp2, which is known to elicit cell death in tomato and tobacco harbouring the *Cf-Ecp2* resistance gene (Laugé et al., 1998), ZtNip2 was identified to contain a putative MD-2-related lipid-recognition domain, hinting at the ability to bind lipids that may have a potential role in innate immunity (Inohara & Nuñez, 2002; Mullen et al., 2003). Furthermore, the onset of ZtNip1 expression during infection matched with necrotic symptom development in planta (Ben M'Barek et al., 2015). Recently, the functional ribonuclease Zt6 was discovered in *Z. tritici* that targets not only plant but also mammalian ribosomal RNA for cleavage in vitro, a feature that makes it highly toxic to wheat, tobacco, bacterial, and yeast cells (Kettles et al., 2018). Intriguingly, the gene expression pattern of Zt6 during infection is marked by a double expression peak. The first boost in expression occurs at 1 day postinfection, followed by down-regulation during the biotrophic life cycle phase. With onset of the necrotrophic phase at 14 days postinoculation, however, Zt6 gene expression increases again (Kettles et al., 2018).

Besides proteinaceous necrosis-inducing agents, secondary metabolite effectors have also been reported to elicit cell death in their host. *C. beticola* is a producer of cercosporin and beticolin, two well-known phytotoxic secondary metabolite effectors. Both toxins are only active in the presence of light and show no host specificity (Daub & Ehrenschaft, 2000; de Jonge et al., 2018; Schlösser, 1962). In multiple *Cercospora* species, targeted gene disruption mutants are unable to produce cercosporin and display reduced virulence, which underlines the importance of necrosis induction for the infection process in this genus (Callahan et al., 1999; Choquer et al., 2005). However, no proteinaceous phytotoxin has been reported for *C. beticola* to our knowledge. In this study, we describe the identification of the first proteinaceous *C. beticola* virulence factor. This protein can induce host cell death in the dark and therefore can complement the light-dependent phytotoxins cercosporin and beticolin. Finally, we find evidence that the gene encoding this virulence factor has evolved under positive selection, possibly reflecting a role in an evolutionary host-pathogen arms race.

## 2 | RESULTS

### 2.1 | Necrosis-inducing activity of *C. beticola* culture filtrate

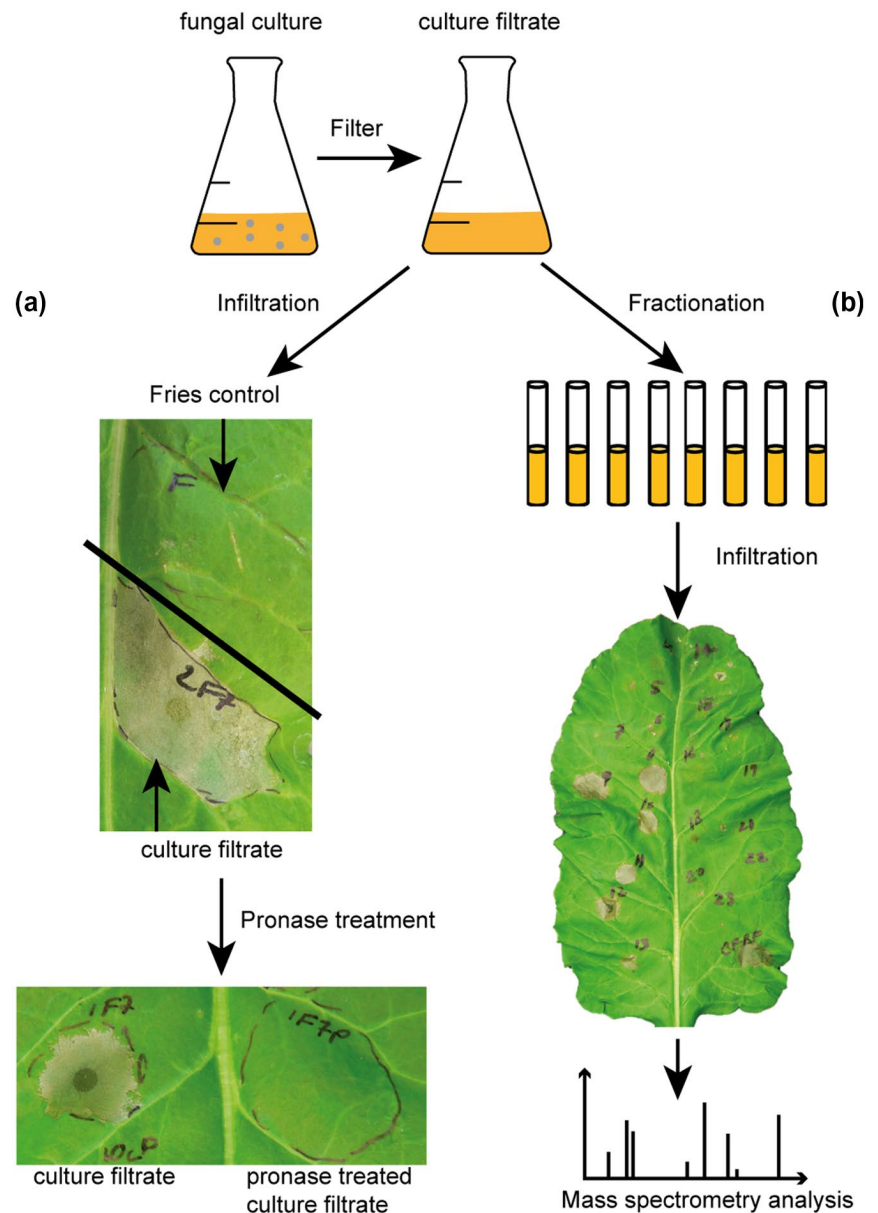
Due to the hemibiotrophic lifestyle of *C. beticola*, we hypothesized that the fungus secretes effector proteins during infection that facilitate disease by causing necrosis and at least a portion of these are produced during in vitro growth. Therefore, we cultured *C. beticola*

in different media (potato dextrose broth [PDB] and Fries medium) and under different conditions (e.g., shaking at 120 rpm or still cultures that were grown without movement, and sampling time points at 3, 5, 7, 12, and 14 days after medium inoculation) in attempts to identify an *in vitro* condition in which effector proteins were produced (Figure 1a,b). All culture conditions were tested for the presence of necrosis-inducing activity by infiltrating culture filtrate into sugar beet leaves (Figure 1a). Ultimately, infiltration of culture filtrate of *C. beticola* grown in Fries medium for 7 days, shaking at 120 rpm, caused clear and repeatable necrosis of the host tissue (Figure 1a). Within 24 hr, the host cells within the infiltration zone had entirely collapsed while cells outside the area remained apparently unharmed. Because *C. beticola* is known to produce cercosporin and beticolin, which are phytotoxic (Daub & Ehrenshaft, 2000; Schlösser, 1962), culture filtrate was treated with a protease mixture to rule out the involvement of phytotoxic secondary metabolites for this necrosis formation. Treatment with proteases abolished necrosis,

confirming that the necrosis-inducing activity can be attributed to a proteinaceous component of the culture filtrate (Figure 1a). To single out the protein responsible for the necrotic phenotype, the active culture filtrate was fractionated using ion exchange chromatography and single fractions were screened for necrosis-inducing activity by individual infiltration into sugar beet leaves (Figure 1b). The fraction that reproducibly caused necrosis was selected for protein identification using tandem mass spectrometry (MS/MS) analysis (Figure S1).

## 2.2 | Effector protein candidate identification

Based on the analysis of MS/MS data and subsequent protein identity searches in the genome of *C. beticola* strain 09-40 (de Jonge et al., 2018), three candidate proteins were identified: CB0940\_03921, CB0940\_10646, and CB0940\_04765. While the



**FIGURE 1** Scheme of the necrosis-inducing effector identification pipeline. A 7-day-old *Cercospora beticola* 09-40 wild-type strain grown in Fries medium was filtered to remove fungal mycelia. (a) When the culture filtrate was infiltrated into 7-week-old sugar beet leaves, a clear necrotic phenotype was observed after 24 hr. Proteolysis treatment eliminated necrosis-inducing activity of the culture filtrate. (b) Culture filtrate was fractionated using ion exchange chromatography and necrosis-inducing activity of individual fractions was assayed by infiltration into sugar beet leaves. All infiltration experiments were repeated at least three times using different sugar beet plants

mature CB0940\_03921 peptide sequence was picked up in full in the MS/MS sample analysis, CB0940\_10646 MS/MS coverage starts with the fifth amino acid of the mature peptide sequence and covers the peptide sequence until the 48th amino acid, totaling 75%. CB0940\_04765 displayed peptide coverage to a total of 73% of the predicted protein sequence. Of these three proteins, only CB0940\_03921 and CB0940\_10646 displayed classic effector characteristics, including secretion signals, high cysteine content (Figure S2), and low molecular weight (9.2 and 6.6 kDa, respectively). In contrast, CB0940\_04765 lacked a signal peptide and contained no cysteines. Analysis of the three candidates with the effector prediction software EffectorP v. 2.0 (Sperschneider et al., 2018) yielded an effector probability score for CB0940\_03921 and CB0940\_10646 of 0.945 and 0.9, respectively. CB0940\_04765 was also predicted to be an effector, with a lower score of 0.557 compared to the other two candidates. Due to the lack of classical effector characteristics and a low predicted effector probability by EffectorP, CB0940\_04765 was therefore excluded from further analysis.

The signal peptide cleavage sites were predicted to be between residues 18 and 19 for CB0940\_03921 and between 16 and 17 for CB0940\_10646 (Figure S2). Furthermore, the six cysteine residues found in the 85 amino acid sequence of the mature CB0940\_03921 protein were predicted to form three disulphide bridges (Figure S2). Although CB0940\_10646 is a rather small protein with 59 amino acids, it is predicted to have four disulphide bonds (Figure S2). On the nucleotide level, each of the two candidate genes had one intron, resulting in a coding sequence of 312 bp for CB0940\_03921 and 228 bp for CB0940\_10646. While no motifs were detectable for CB0940\_03921, CB0940\_10646 contains an AxxxG motif that may be involved in dimerization (Kairys et al., 2004). Additionally, a SxxV(K/R) motif associated with monocation specificity ( $\text{Cu}^+$ ,  $\text{Ag}^+$ , and  $\text{Au}^+$ ) was also detected (Bird et al., 2013; Changela et al., 2003) (Figure S2). While a SxxV(K/R) motif was previously reported to occur in combination with a CxGxxxxDCP metal-binding loop, CB0940\_10646 appears to only be harbouring the monocation specificity domain without the metal-binding loop motif. Notably, CB0940\_03921, located on chromosome 4, is found on the edge of a contiguous sequence stretch and is thus flanked by a large sequence gap, a phenomenon typically observed for effector genes as a consequence of close association with transposable elements that are notoriously more difficult to assemble (Figure S3) (Thomma et al., 2016).

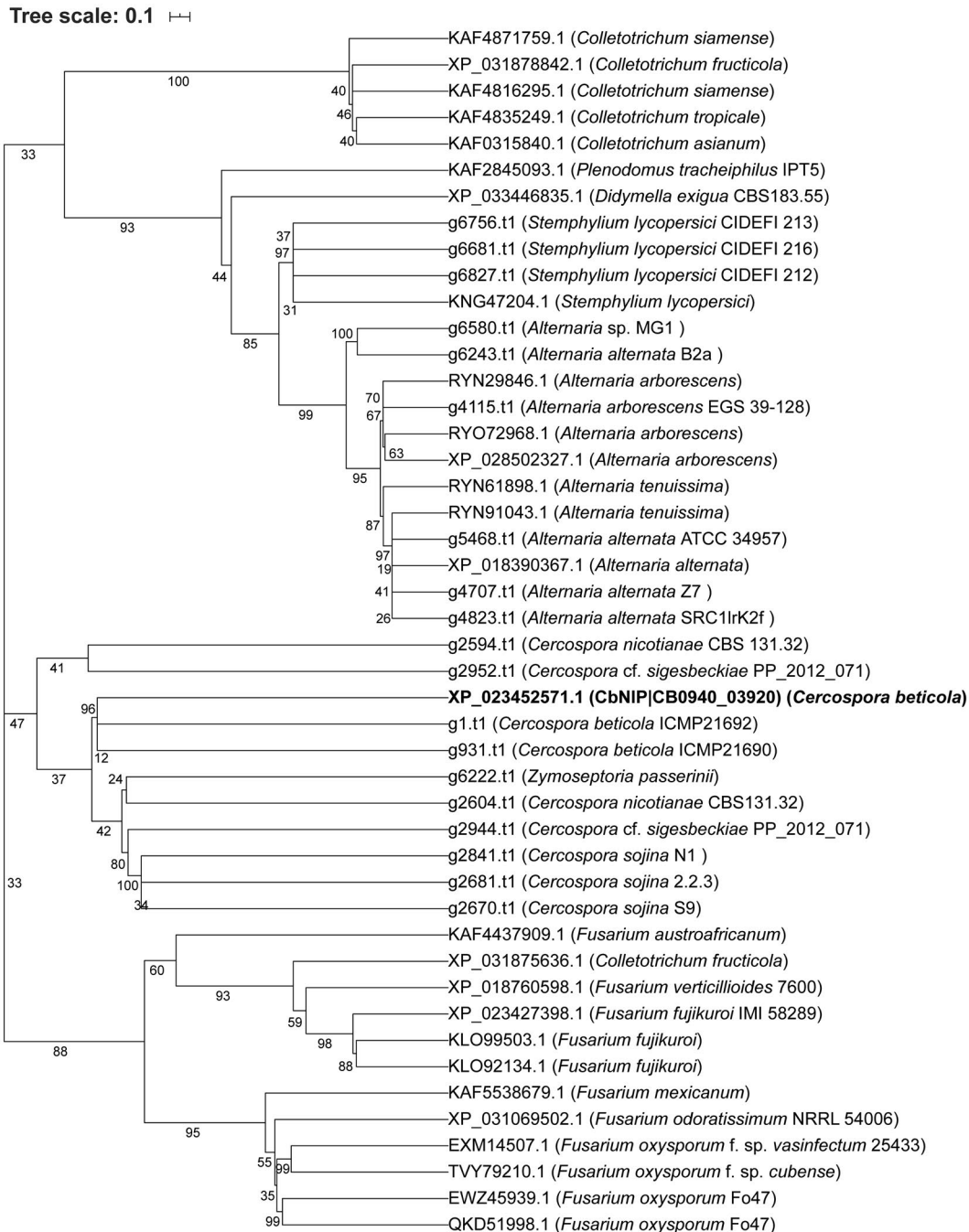
### 2.3 | Protein sequence homology

While searching for potential homologs of our two effector candidates, two homologous hypothetical proteins from *Colletotrichum* spp. (CNYM01\_08238 and CSIM01\_12439) were identified for CB0940\_10646 when queried by NCBI BLASTp ( $E < 10^{-6}$ ) against the nonredundant (NR) database (Table S1). No homologs were identified in the UniprotKB/Swiss-Prot database consisting of functionally characterized proteins. NCBI tBLASTn analysis ( $E < 10^{-6}$ ) against

fungal genome sequences also did not yield additional candidate homologous proteins. For CB0940\_03921, we were able to identify 26 homologs via NCBI BLASTp ( $E < 10^{-6}$ ) against the NR database in several fungi in addition to *C. beticola*, specifically *Alternaria* spp., *Fusarium* spp., *Colletotrichum* spp., *Stemphylium lycopersici*, *Didymella exigua*, and *Plenodomus tracheiphilus* (Figure 2 and Table S2). In addition, we identified multiple candidate CB0940\_03921 homologs in unannotated fungal genome sequences, specifically those belonging to *Cercospora* and *Alternaria* spp. and in *S. lycopersici* and *Zymoseptoria passerinii* (Table S2). CB0940\_03921 (hereafter described as CbNip1 for necrosis-inducing protein 1) homologs found in *C. beticola* strains clustered together (Figure 2) and showed high sequence conservation (Figure S4). One *C. beticola* strain (ICMP21690) appears to encode two CbNip1 copies with identical amino acid sequences (amino acid sequences of CbNip1 homologs can be accessed in Dataset S1), but detailed inspection of the ICMP21690 genome suggests this is most likely the result of erroneous genome assembly as it appears that the encoding contig (PDU101000001.1) is represented by a near-perfect head-to-head palindrome. Notably, we identified two, probably genuine, CbNip1 copies in *Cercospora nicotianae* and in *Cercospora cf. sigesbeckiae* (Dataset S1). In this case one paralog (g2604.t1 for *C. nicotianae* and g2944.t1 for *C. cf. sigesbeckiae*) clusters with *C. beticola* CbNip1 and several other *Cercospora* spp. CbNip1 homologs and the only remotely similar homolog in the barley pathogen *Z. passerinii* (Figure 2). The other paralogs (g2594.t1 for *C. nicotianae* and g2952.t1 for *C. cf. sigesbeckiae*, further referred to as CbNip1-like) form a separate cluster and are more distant from CbNip1 (Figure 2). The two paralogs are spatially close on both the *C. nicotianae* (POSS01000015.1: 305,923-306,288; POSS01000015.1: 279,073-279,458) and the *C. cf. sigesbeckiae* genomes (NKQR01000009.1: 123,018-123,382; NKQR01000009.1: 147,878-148,249) at c.25 kb, suggesting a potentially ancestral organization that is further supported by the identification of a similar arrangement in *Cercospora kikuchii* strain ARG\_18\_001 and in *Cercospora citrullina* strain Cer139-09 following tBLASTn analysis using the CbNip1 and CbNip1-like protein as queries. Careful analysis of the *C. beticola* genome revealed a predicted pseudogenized CbNip1-like copy (i.e., with several in-frame stop codons) distant from CbNip1 on chromosome 4. All homologs, except those in *Fusarium fujikuroi* (KLO92134.1, KLO99503.1, and XP\_023427398.1) and in *Colletotrichum asianum* (KAF0315840.1), encode a predicted signal for secretion and encompass the previously mentioned six, similarly spaced, conserved cysteine residues (Figure S5).

### 2.4 | CbNip1 protein structure homology

To gain insight into the biological function of CbNip1, we used the I-TASSER server (Roy et al., 2010; Yang et al., 2015; Zhang, 2008) to predict the three-dimensional structure of identified Nip1 proteins in *C. beticola* (XP\_023452571.1), *C. nicotianae* (g2604.t1), *C. cf. sigesbeckiae* (g2944.t1), and *Cercospora sojina* (g2841.t1). When evaluating putative secondary structure, the most similar structure



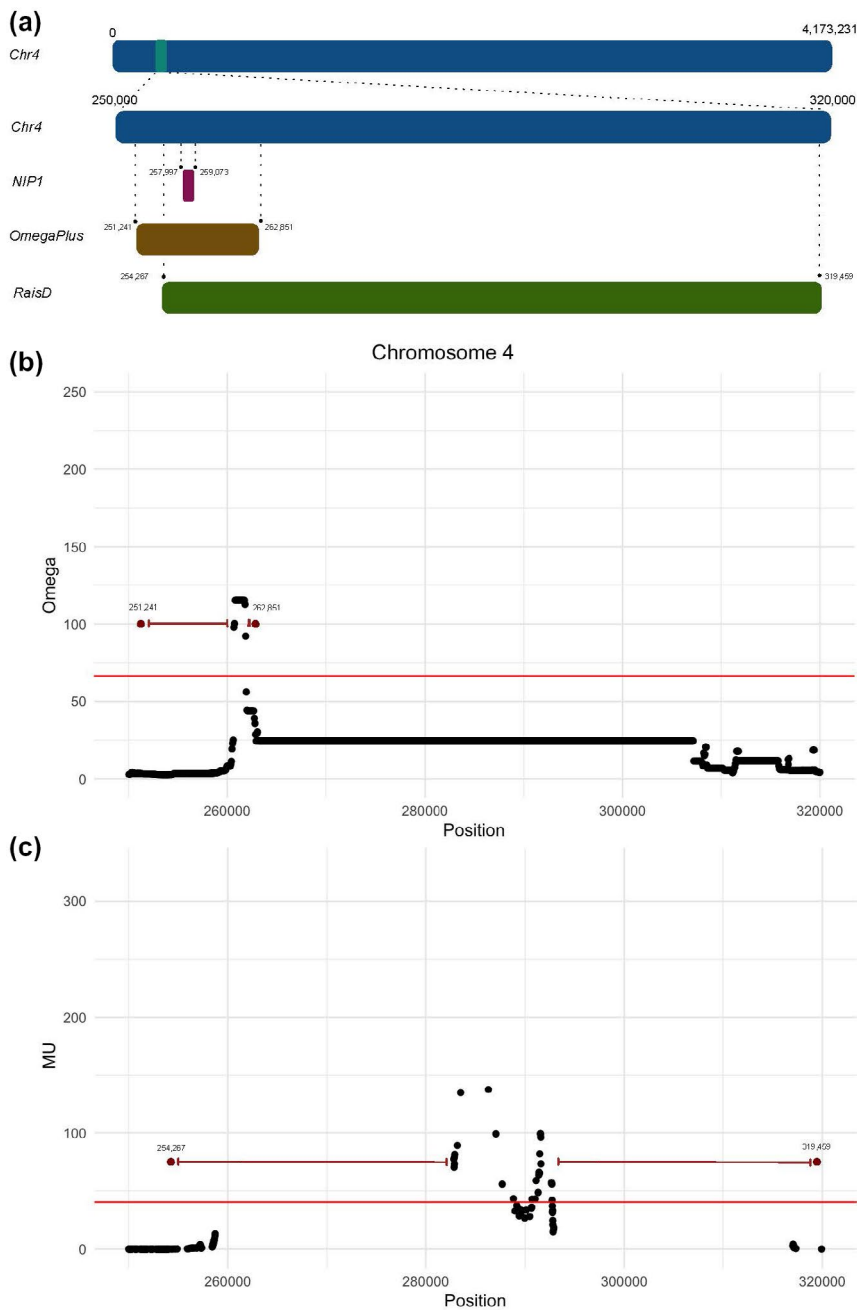
**FIGURE 2** Phylogeny of CbNip1 and CbNip1 homologs found in *Alternaria* spp., *Stemphylium lycopersici*, *Zymoseptoria passerinii*, and different *Cercospora* species. The tree was constructed using the 46 proteins homologous to CbNip1. Peptide sequences were aligned using MAFFT (with default options) and subsequently filtered for phylogenetically relevant columns with trimAl. A maximum-likelihood tree was built using automated protein model selection and 100 rapid bootstraps. The rooted tree was visualized in iTOL

to *C. beticola* CbNip1 was *C. nicotianae* with two highly conserved predicted  $\alpha$ -helices (not shown). However, the predicted  $\beta$ -strand regions were more conserved between *C. nicotianae*, *C. cf. sigesbeckiae*, and *C. sojina* proteins. The highest confidence protein model amongst the *Cercospora* spp. was for *C. beticola* Nip1 (confidence score [C-score] = -1.7; Table S3 and Figure S6). The top protein model for each species, except *C. sojina*, showed closest structural homology to the  $\beta$  subunit of the KP6 killer toxin encoded by Ustilago maydis virus P6 (Table S3). *C. sojina* Nip1 had the lowest confidence

protein model (C-score = -3.84). Low C-scores and disparate predictions between Nip1 proteins were obtained for ligand binding and enzymatic activity, making any inference of function difficult.

## 2.5 | CbNip1 gene variation

We next investigated the *CbNip1* gene sequence within 190 North American *C. beticola* isolates primarily sampled from North Dakota and



**FIGURE 3** The genomic region encoding *CbNip1* colocalizes with a selective sweep. Genome-wide screen of selective sweeps in *Cercospora beticola* revealed a candidate region on chromosome 4 that spans the *CbNip1* locus. (a) Position of the *CbNip1* gene on chromosome 4 and the regions that were identified by the selective sweep analyses using demographic modelling and methods implemented in the programs Omega and RAiSD. (b) OmegaPlus and (c) RAiSD candidate regions on the chromosome arm of chromosome 4. The significance thresholds of the  $\mu$  and  $\omega$  statistics were determined with demographic simulations. Successive windows that were identified as significant were merged. The points in red represent the most left and the most right variants of the significant successive windows of the two statistics  $\omega$  and  $\mu$  computed by OmegaPlus and RAiSD, respectively

Minnesota to assess the extent of within-species variation in the gene (Spanner et al., unpublished data). In total, three different *CbNip1* coding region haplotypes were identified. Most isolates ( $n = 189$ ) had an identical *CbNip1* sequence to the reference isolate 09-40. Six strains harboured a synonymous mutation at codon D21 and the amino acid change N94H when compared to the reference haplotype. One strain had a single synonymous mutation at codon P41.

## 2.6 | Genomic region encoding *CbNip1* recently underwent a selective sweep

A selective sweep occurs when a beneficial mutation increases in frequency and becomes fixed in the population. The genomic signature of such positively selected mutations is a genomic region

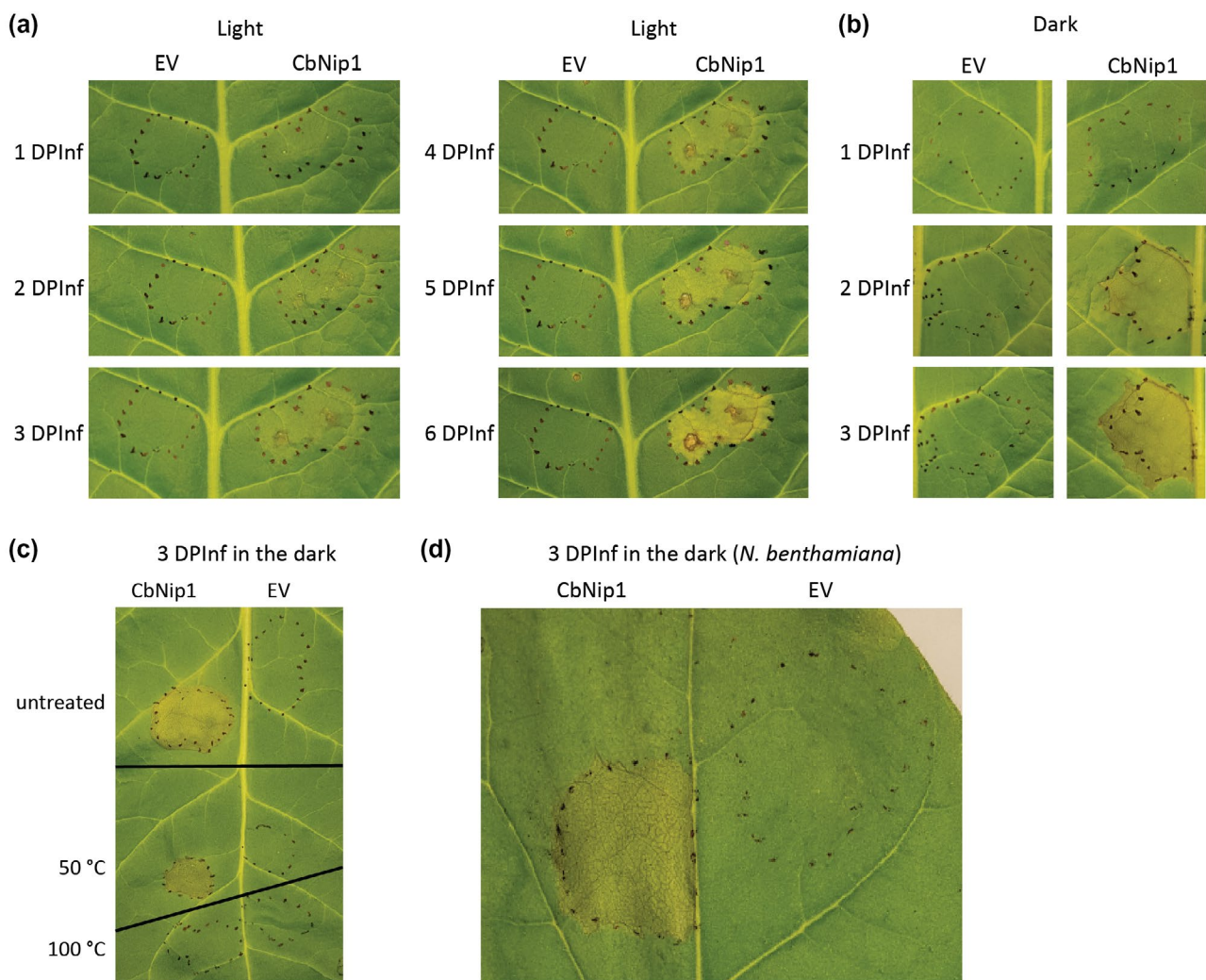
deprived of variation and with a high linkage disequilibrium. The “selective sweep map” of *C. beticola* was generated from a population genomic data set using 89 DMI-resistant North American sugar beet-infecting *C. beticola* isolates (Spanner et al., unpublished data). We correlated the genomic positions of the genes encoding *CbNip1* homologs in *C. beticola* with the selective sweep map. In brief, the analysis used the site frequency spectrum (SFS) of genetic variants in the population genomic data sets with demographic simulations to assess the significance of outlier loci with deviations from the expected SFS under neutrality. Two independent approaches were used to detect outlier loci deviating from the expected distribution under neutrality: OmegaPlus and RAiSD (Alachiotis & Pavlidis, 2018; Alachiotis et al., 2012). Both programs detected an outlier locus at the end of chromosome 4 that spans the *CbNip1* gene (Figure 3). This locus showed significantly higher values of both the two statistics  $\omega$

(extent to which average linkage disequilibrium is increased on each side of the selective sweep) and  $\mu$  (mutation rate per site per individual) as computed by OmegaPlus and RAiSD, respectively, when compared to values obtained from simulations under a neutral demographic scenario. The regions detected with the two methods include 10,750 bp (OmegaPlus) and 65,192 bp (RAiSD), and comprise 2,754 and 6,118 single nucleotide polymorphisms (SNPs), respectively (Figure 3).

## 2.7 | Heterologous expression of effector protein candidates and phenotype upon infiltration

To further characterize the candidate necrosis-inducing effectors, the mature CbNip1 protein was produced heterologously

in *Escherichia coli* and infiltrated into sugar beet leaves that were subsequently kept in a growth chamber with a 10-hr light cycle. Unlike the response from the culture filtrate, no phenotype was observed for CbNip1 at 1 day postinfiltration (DPIInf) (Figure 4a). However, after 2 DPIInf the infiltration area of CbNip1 started to appear slightly chlorotic while the empty vector control remained unchanged (Figure 4a). Chlorosis of the CbNip1-infiltrated area increased over time until it turned necrotic (Figure 4a). Because light is critical for the activity of *C. beticola* secondary metabolite effectors cercosporin and beticolin and has also been shown to be essential for functionality of other necrosis-inducing factors (Ben M'Barek et al., 2015), we questioned whether light may play a role in the activity of CbNip1. To evaluate this, we infiltrated CbNip1 into sugar beet leaves that were subsequently placed in a growth chamber with



**FIGURE 4** Necrosis-inducing phenotype of CbNip1 protein. (a) Chlorosis/necrosis development after infiltration of CbNip1 into sugar beet leaf exposed to a 10 hr/14 hr light/dark cycle for up to 6 days postinfiltration (DPIInf) and empty vector sample (EV) infiltration served as a control. (b) Necrosis development after infiltration of CbNip1 into a sugar beet leaf kept in 24 hr darkness and an EV infiltration that served as a control. (c) Treatment of CbNip1 and EV exposed to 50 °C for 30 min did not affect necrosis-inducing activity of CbNip1 while treatment of both samples at 100 °C for 30 min abolished necrosis induction. Untreated samples served as controls. (d) Necrosis formation after infiltration of CbNip1 into a *Nicotiana benthamiana* leaf. An EV control sample served a control. All infiltration experiments were repeated at least three times using different sugar beet plants

different light/dark conditions (24 hr light, 10 hr light/14 hr dark cycle, 24 hr darkness). Of these growth chamber regimes, only incubation of *CbNip1* infiltrated leaves incubated in 24 hr darkness resulted in clear necrosis of the complete infiltration area by 3 DPI (Figure 4b). To assess the stability of *CbNip1*, we incubated the protein and empty vector control at 50 °C or 100 °C for 30 min, after which proteins were infiltrated into sugar beet leaves and subsequently shielded from light exposure. While exposure to 100 °C abolished necrosis formation, samples treated with 50 °C were still able to cause necrosis (Figure 4c). Furthermore, infiltrations of *CbNip1* into *Nicotiana benthamiana* led to the same necrotic phenotype, indicating that the *CbNip1* mode of action is not host-specific (Figure 4d).

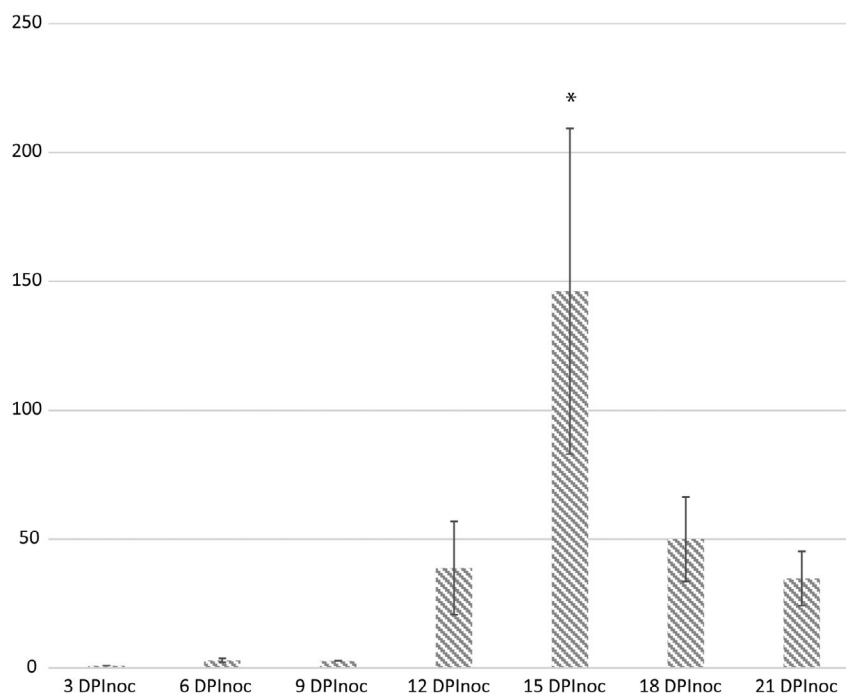
We were unable to produce CB0940\_10646 in sufficient amounts in either *Pichia pastoris* or *E. coli*. Therefore, chemically synthesized CB0940\_10646 protein was used for infiltration into sugar beet leaves. In contrast to *CbNip1*, no phenotype was visible for the conditions tested, which included light/dark exposure, refolding of the protein, and the supplementation of trace elements (Figure S7). Consequently, CB0940\_10646 was excluded from further analysis.

## 2.8 | In planta gene expression profile of *CbNip1* matches necrotic lesion development

To determine the expression pattern of *CbNip1* during *C. beticola* colonization, we inoculated sugar beet plants with a *C. beticola* wild-type strain and harvested leaf samples at 3, 6, 9, 12, 15, 18, and 21 days postinoculation (DPI). Gene expression analysis revealed that *CbNip1* is minimally expressed at early time points (Figure 5). However, from 12 DPI onwards *CbNip1* expression increased until peaking at 15 DPI. Interestingly, onset of *CbNip1* up-regulation at 12 DPI matched symptom development on the sugar beet leaves (Figure S8). At 15 DPI, many single necrotic spots were visible while *CbNip1* expression reached its peak. However, with progressing necrosis expansion in planta, *CbNip1* experienced a steady down-regulation again from 18 DPI onwards (Figure 5).

## 2.9 | *CbNip1* is a virulence factor

To investigate whether *CbNip1* is required for full *C. beticola* virulence, we generated  $\Delta CbNip1$  mutants and inoculated sugar beet



**FIGURE 5** *CbNip1* gene expression during *Cercospora beticola* infection on sugar beet. Gene expression profile of *CbNip1* during *C. beticola* wild-type strain 09-40 infection course at 3, 6, 9, 12, 15, 18, and 21 days postinoculation (DPI). *CbNip1* gene expression was normalized to *C. beticola actin* gene expression. The relative gene expression (displayed on the y axis) of three biological repetitions was calculated in comparison to the earliest measured time point using the Pfaffl method (Pfaffl, 2001). Error bars indicate the standard error of three biological replicates. By performing a one-way analysis of variance (ANOVA) ( $p < .05$ ) with a post hoc Tukey test, we tested for differences between the gene expression levels of different time points. A significant difference can be observed between 3, 6, and 9 DPI when compared to 15 DPI ( $p < .05$ , indicated by an asterisk). However, between 12 and 15 DPI there is no significant difference and also later time points such as 18 and 21 DPI do not show a significant difference to 15 DPI. This suggests an increase in *CbNip1* gene expression at 12 DPI compared to earlier time points (3–9 DPI), but with an expression lower than the gene expression at 15 DPI. Furthermore, the loss of significance after 15 DPI suggests *CbNip1* expression decreases again at later time points (18 and 21 DPI)



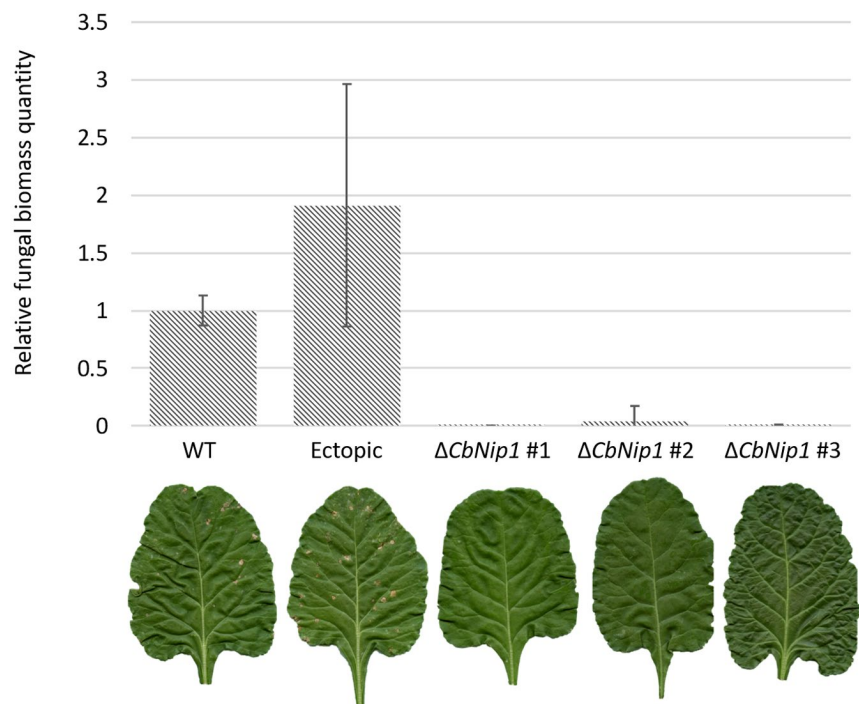
plants with wild-type *C. beticola*, three individual  $\Delta CbNip1$  mutants (Figure S9), and an ectopic mutant (Figure S10). To ensure that the generated  $\Delta CbNip1$  mutants did not suffer any fitness penalties, the growth of the 09-40 wild type strain and the three  $\Delta CbNip1$  mutants was assessed under in vitro growth conditions (Figure S11). No growth deficiency was detected between the wild-type and mutant strains when grown on potato dextrose agar (PDA) and PDA amended with charcoal (0.01 g/ml), different cell wall (Calcofluor 100  $\mu\text{g/ml}$  or Congo red 45  $\mu\text{g/ml}$ ), osmotic (1 M sorbitol or 1 M NaCl), or oxidative stressors (1 mM  $\text{H}_2\text{O}_2$ ) (Figure S11). In addition to visible symptom assessment in planta, fungal biomass was measured using quantitative PCR (qPCR) for each treatment individually to determine the level of fungal colonization of the host plants. While clear infection symptoms were displayed by sugar beet plants inoculated with wild-type *C. beticola* or the *CbNip1* ectopic mutant, highly reduced symptom formation was observed for plants inoculated with any of the three individual  $\Delta CbNip1$  strains (Figure 6). In agreement with the noticeable difference in the in planta phenotype of wild-type/ectopic mutant and  $\Delta CbNip1$  strains, evaluation of fungal biomass showed reduced fungal colonization in plants infected with  $\Delta CbNip1$  compared to high levels of fungal biomass found in sugar beet plants inoculated with the wild-type *C. beticola* strain and the ectopic mutant (Figure 6).

### 3 | DISCUSSION

*C. beticola* is a hemibiotrophic fungus that is dependent on necrosis formation during infection (Weltmeier et al., 2011) and known to use the secondary metabolite effector cercosporin to cause host cell death (Daub & Ehrenschaft, 2000). Here, we report the identification

of the *C. beticola* necrosis-inducing effector CbNip1. By searching for in vitro parameters that trigger *C. beticola* to secrete effector proteins, we found growth conditions under which *C. beticola* produces proteinaceous effectors that cause necrosis on infiltration into sugar beet leaves within 24 hr. While infiltration of pure CbNip1 into sugar beet leaves took 48 hr to lead to visible necrosis, the timing difference in necrosis formation is probably due to the presence of multiple necrosis-inducing effectors besides CbNip1 in the culture filtrate. Besides CbNip1, fractionation of the culture filtrate with subsequent mass spectrometry analysis of the necrosis-inducing fraction identified the presence of two other proteins, CB0940\_10646 and CB0940\_04765, of which CB0940\_04765 was excluded for further analysis due to the lack of typical effector characteristics.

For functional analysis, CbNip1 was heterologously produced and infiltrated into sugar beet leaves. As mentioned above, we found that the full potential of CbNip1 to induce host cell death was dependent on the absence of light. Light is known to influence *Cercospora zea-maydis* infection capability as the ability to find stomata and form appressoria is abolished in the dark (Kim et al., 2011). Plants are also impacted by light in various ways, including alteration of leaf physiology (Kami et al., 2010; Roberts & Paul, 2006). Furthermore, studies on host resistance responses have demonstrated that light is required for the full cascade of plant resistance responses (Guo et al., 1993; Roberts & Paul, 2006; Roden & Ingle, 2009). Based on microarray expression profiling of the *C. beticola*-sugar beet interaction, 571 sugar beet genes were induced, including pathogenesis-related (PR) genes and genes involved in lignin and alkaloid biosynthesis at the onset of necrotic symptom formation (Weltmeier et al., 2011). While the products of these defence-associated genes could potentially impede CbNip1 function in the presence of light, PR genes have been shown to be repressed in the dark (Guo et al., 1993; Roberts



**FIGURE 6** Fungal biomass quantification of *Cercospora beticola* 09-40 wild-type strain, three individual  $\Delta CbNip1$  mutants, and one ectopic transformant. Sugar beet plants inoculated with *C. beticola* strains at 21 days postinoculation with photographs showing respective disease severity below. Gene expression was quantified with SbEc1-F/SbEc1-R quantitative PCR (qPCR) primers for sugar beet and CbActin Fp/CbActin Rp qPCR primers for *C. beticola*. Error bars represent standard error of three biological replicates. Fungal biomass was calculated using the  $\Delta\Delta C_t$  method relative to the average value of the wild-type inoculated sugar beet plants

& Paul, 2006; Roden & Ingle, 2009). However, a recent paper on effector-triggered immunity in a bacteria–plant interaction mentions that hypersensitive responses (HRs) caused by effector recognition via a nucleotide-binding leucine-rich repeat (NB-LRR) immune receptor were more pronounced in the dark (Qi et al., 2018). While necrotrophic effectors such as SnTox1 have been reported to exploit interactions with defence-associated genes such as specific plant receptors to induce cell death in the host specifically (also known as reverse gene-for-gene interaction) (Liu et al., 2004; Shi et al., 2016), in the case of CbNip1 necrosis is not only induced in sugar beet but also in the nonhost *N. benthamiana*. Therefore, CbNip1-triggered induction of necrosis via interaction with a corresponding receptor protein would require that this receptor is conserved among various plant species. Given that ample predicted secondary structure similarity was seen between CbNip1 and *C. nicotianae* CnNip1 through I-TASSER protein modelling (Roy et al., 2010; Yang et al., 2015; Zhang, 2008), the protein structure may be conserved enough between CbNip1 and CnNip1 such that CbNip1 can interact with the same target in the nonhost plant *N. benthamiana*.

Besides cell death through recognition, CbNip1 function may be the result of general toxicity to plants. For example, some effectors modulate targets in their host but potentially also in other plants for necrosis induction. This mode-of-action has been observed for the small sRNase Zt6 of *Z. tritici*, which displays universal cytotoxicity by cleaving plant and mammalian ribosomal RNA (Kettles et al., 2018). Nevertheless, necrosis formation could also be the result of cell wall-degrading enzyme activity as cell wall-degrading enzymes of various fungal pathogens have been found to be essential for fungal virulence (Bailey et al., 1990; Brito et al., 2006; Kars et al., 2005).

Protein modelling of Nip1 revealed that the closest structural analog to Nip1 from *C. beticola*, *C. nicotianae*, and *C. cf. sigesbeckiae* is the  $\beta$  subunit of the KP6 killer toxin produced by *Ustilago maydis* virus P6 (KP6 $\beta$ ). Double-stranded RNA totiviruses can infect certain strains of the corn smut fungus *Ustilago maydis* (Allen et al., 2013). These viruses produce potent antifungal proteins called “killer toxins” that are secreted by the host and kill competing uninfected strains of *U. maydis* (Koltin & Day, 1975). The KP6 toxin is one such killer toxin and is a heterodimer composed of two subunits: KP6 $\alpha$  and KP6 $\beta$  (Allen et al., 2013). The KP6 $\alpha$  and KP6 $\beta$  subunits have high structural similarity, but KP6 $\beta$  is responsible for cytotoxic activity via an unknown mechanism (Finkler et al., 1992). It is possible that Nip1 has similar cytotoxic activity, which causes the necrosis seen in leaf infiltrations of sugar beet and *N. benthamiana*.

Using population genomic data from a North American population of *C. beticola* isolates, we found evidence that the *CbNip1* locus resides in a genomic region that has recently experienced a selective sweep. A selective sweep occurs when a favourable mutation appears in a population and becomes fixed as a result of its fitness advantage. Genetic variants in the same genomic background as the beneficial mutation will “hitchhike” with the selected mutation. This leaves a footprint at the genomic locus characterized by reduced variation and high linkage disequilibrium compared to distal

genomic regions (Smith & Haigh, 1974). The identification of *CbNip1* within such a selective sweep region underscores the importance of this effector in the population. However, the nature of the selection pressure to retain *CbNip1* remains unclear. The selection of this gene variant within this population could be the result of a conserved and specific host target that was widely introduced in sugar beet germplasm. For example, given the necrotic phenotype of *CbNip1*, it is tempting to speculate that this effector specifically interacts with a recently introgressed host immune receptor in a reverse gene-for-gene interaction, as known from other systems (Faris et al., 2010; Friesen et al., 2007, 2008; Shi et al., 2016). It is possible that the beneficial mutation that conferred a selective sweep in the *CbNip1* region relates to regulation of gene expression. We speculate that the late onset of *CbNip1* gene expression could be an adaptation to the necrotrophic stage of the pathogen. For example, there may have been directed evolution for *CbNip1* to be expressed and recognized by sugar beet solely during its necrotrophic phase as a means of facilitating fungal growth. This may also explain cell death in nonhost plants upon infiltration with the *CbNip1* protein where the necrotic response could be due to a defence-inducing activity as seen in other necrotrophic fungal pathogens on nonhosts (Kettles et al., 2017; Raffaello & Asiegbu, 2017). Alternatively, *CbNip1* may not have a host target and therefore its nonhost specificity is due to the general cytotoxic nature of this protein. Further investigation into nonhost responses to *CbNip1* would be necessary to reveal a mechanism for the *CbNip1*-induced necrotic phenotype.

While a necrotic phenotype is observed for *CbNip1*, the other effector candidate CB0940\_10646 failed to induce any phenotype under tested conditions. Because CB0940\_10646 has domains associated with dimerization and monocation specificity, the inability to induce necrosis may be due to the absence of a cognate cofactor. As CB0940\_10646 was chemically synthesized, it is possible that due to its monocation specificity-associated domain, the addition of trace elements (including copper) as present in the Fries medium of the initial culture filtrate might activate CB0940\_10646 function. However, the supplementation of metal ions to CB0940\_10646 did not lead to phenotype formation in sugar beet leaves. Moreover, infiltration of CB0940\_10646 with *CbNip1* did not obviously enhance *CbNip1*-induced necrosis. Further research is required to identify the allied cofactors for CB0940\_10646, if any.

In accordance with *CbNip1* necrosis-inducing ability, we have found that necrotic symptom development in planta correlates with up-regulation of *CbNip1* expression (Figure 5 and Figure S8). Induction of host necrosis during the biotrophic phase is not likely beneficial for the fungus, therefore it is not surprising that *CbNip1* is minimally expressed at early infection time points (3–9 DPI<sub>noc</sub>). An increase in *CbNip1* expression and the development of necrotic lesions occurred simultaneously, suggesting that *CbNip1* is linked to the switch from biotrophic to necrotrophic lifestyle of the fungus. Once necrosis formation is ongoing and existing necrotic lesions start to fuse, *CbNip1* expression is reduced again to a similar level as observed in the initial cell death induction phase at 12 DPI<sub>noc</sub>,

indicating that necrosis induction by CbNip1 may still be important at later time points. Interestingly, the *CbNip1* expression pattern is similar to expression patterns of other necrosis-inducing effectors from different protein families found in the hemibiotroph *Z. tritici*. *ZtNip1* showed an expression pattern where gene up-regulation matched onset of symptom development in planta (Ben M'Barek et al., 2015). Similarly, the *Z. tritici* Nep-1-like protein gene *MgNip* peaked towards the end of the biotrophic phase before necrotic lesions were visible (Motteram et al., 2009). However, there are also examples of contrasting expression patterns to *CbNip1*. For example, the expression of *Zt6* in planta is characterized by a double peak probably attributed to a double functionality (Kettles et al., 2018).

Because *C. beticola* requires necrotic plant tissue to complete its life cycle (Weltmeier et al., 2011), we determined whether CbNip1 was also essential for fungal virulence. We found that site-directed  $\Delta$ *CbNip1* mutants are impeded in virulence compared to the wild-type *C. beticola* strain and an ectopic mutant strain. Not only did plants inoculated with  $\Delta$ *CbNip1* mutants develop fewer *C. beticola*-specific lesions, biomass determination revealed there was less fungal biomass in plant tissue compared to the progenitor wild type (Figure 6). Taken together, this indicates that CbNip1 plays an important role in *C. beticola* virulence. As mentioned earlier, *C. beticola* produces the secondary metabolite cercosporin and a family of phytotoxins called beticolins, both of which are able to cause cell death in the presence of light (Daub & Ehrenshaft, 2000; Jalal et al., 1992; Schlösser, 1962; Yamazaki et al., 1975) and cercosporin was shown to be a virulence factor for several *Cercospora* species (Callahan et al., 1999; Choquer et al., 2005). Because light activation is essential for cercosporin and beticolin functionality, they are probably not active in the dark. With the secretion of CbNip1, however, *C. beticola* may be defying this light-associated limitation using additional necrosis-inducing agents to cover both light and dark conditions to achieve maximal host cell death to complete its life cycle.

In conclusion, we have shown that *C. beticola* secretes the effector protein CbNip1 during infection that in the absence of light has the ability to cause necrosis on infiltration into sugar beet leaves within 48 hr. Furthermore, *CbNip1* expression in planta correlates with necrotic symptom appearance during *C. beticola* sugar beet infection. Targeted gene replacement of *CbNip1* led to a reduction in virulence, indicating that CbNip1 is a virulence factor for *C. beticola*. As CbNip1 has no obvious homology to other characterized proteins in public databases, future studies will be directed to identify CbNip1 mode of action. Studies on pathogen–host plant interactions often focus on processes that occur in light conditions, but it may be interesting to understand how this interaction is altered in the dark, a vital condition for unhampered CbNip1 function. Consequently, CbNip1 is a fungal virulence factor that is hypothesized to take advantage of the reduced host plant defence response level due to the absence of light. Further analysis of yet unknown functional motifs of CbNip1 as well as localization studies will help to shed light on the biology of CbNip1.

## 4 | EXPERIMENTAL PROCEDURES

### 4.1 | Fungal strains

*C. beticola* wild-type strain 09-40 was isolated from leaf material collected from a sugar beet field in the Red River Valley, USA in 2009. The fungus was kept at 22 °C on PDA (Difco) and fungal site-directed gene deletion mutants in a 09-40 background on PDA amended with 150  $\mu$ M hygromycin B (Duchefa).

### 4.2 | Culture filtrate preparation and infiltration

A 5 mm plug was taken from the actively growing zone of *C. beticola* wild-type strain 09-40 on PDA and used to inoculate a 250 ml conical flask filled with 100 ml of Fries medium (Friesen & Faris, 2012). After 7 days of incubation at 120 rpm under 24-hr light conditions at 21 °C, the liquid culture was run through two layers of Miracloth (EMS Millipore Corp.) to filter out fungal mycelia and subsequently filter-sterilized with a 0.45  $\mu$ m Filtropur membrane (Sarstedt). Approximately 30–50  $\mu$ l of sterile culture filtrate was infiltrated into the leaves of 7-week-old sugar beet plants of the variety C093 (formerly 86RR66) using a 1 ml needleless syringe. Infiltration experiments were repeated at least three times with multiple individually produced culture filtrates. Plants were kept in a greenhouse chamber with an average temperature of 26 °C during the day and approximately 17 °C during the night. Chambers were equipped with additional lighting to ensure 16 hr of light a day. To confirm the proteinaceous nature of the necrosis-inducing agent, 50  $\mu$ l of 3-(*N*-morpholino)propanesulfonic acid (MOPS) buffer (1 M, pH 7.5) and 25  $\mu$ l of pronase (1 mg/ml) (Sigma) or water as control was added to 425  $\mu$ l of culture filtrate and incubated at 22 °C for 4 hr. Subsequently, samples were infiltrated into sugar beet leaves as described above.

### 4.3 | Culture filtrate fractionation

Culture filtrate was partially purified as described in Liu et al. (2009). In short, 100 ml of 7-day-old *C. beticola* wild-type strain 09-40 grown in Fries medium was first filter-sterilized and then dialysed against water using a 3.5 kDa molecular weight cut-off dialysis membrane (Fisher Scientific). The next day, the dialysed culture filtrate was loaded onto a HiPrep SPXL 16/10 cation exchange column (GE Healthcare) using the ÄKTA prime plus (GE Healthcare) liquid chromatography system. After a washing step with 50 ml of 20 mM sodium acetate buffer pH 5.0, 5 ml fractions were collected during gradient elution of 0–300 mM NaCl plus 20 mM sodium acetate pH 5.0 at a flow rate of 5 ml/min over 20 min. Collected fractions were individually infiltrated into 7-week-old sugar beet plants of the variety C093 and screened for necrotic phenotype. Fractionation and infiltration experiments were repeated at least three times.

#### 4.4 | Preparation of necrosis-inducing protein fraction for MS/MS analysis

The fraction that repeatedly caused necrosis was loaded onto a pre-cast 16.5% Tris-Tricine polyacrylamide gel (Bio-Rad). Protein spots were excised and sent to the Center for Mass Spectrometry and Proteomics at the University of Minnesota for trypsin digestion and subsequent LC-MS analysis. Peptide mass fingerprints and peptide sequence information were used to search for protein identity using the annotated *C. beticola* 09-40 genome (de Jonge et al., 2018).

#### 4.5 | gDNA extraction, RNA extraction, and cDNA synthesis

Genomic DNA was extracted using a modified version of the microprep protocol published by Fulton et al. (1995), replacing chloroform:isoamyl alcohol (24:1 vol/vol) with phenol:chloroform:isoamyl alcohol (25:24:1 vol/vol/vol).

RNA extraction followed the TRIzol method (Ambion) according to the manufacturer's protocol and subsequently cleaned up three times using the RNase-free DNase set (Qiagen) according to Appendix E of the RNase Mini Handbook 06/2012. For cDNA synthesis, 1 µg of total RNA was used with the SuperScript III reverse transcriptase kit (Invitrogen) following the manufacturer's protocol.

#### 4.6 | Sequence analysis

CbNip1 homologs were identified online via NCBI BLASTP and tBLASTn analysis of annotated and unannotated whole-genome sequences, respectively. Selected homologous sequences identified via tBLASTn analyses were subsequently extracted via local ab initio gene prediction of the corresponding genome sequence using the Augustus training parameters previously prepared for *C. beticola* (de Jonge et al., 2018). For phylogenetic analysis of CbNip1 and CbNip1 homologs (Table S2) and phylogenetic tree analysis we aligned all CbNip1 homologs by MAFFT v. 7.310 (Katoh & Standley, 2013) (setting: *--auto*), then filtered the alignment using trimAl v. 1.4.rev22 (Capella-Gutiérrez et al., 2009) (settings: *-gt 0.9 -cons 60* [remove all positions with gaps in 10% or more sequences, unless it leaves less than 60% of original alignment in which case the 60% best is reported]). The maximum-likelihood (ML) phylogenetic tree including bootstrapping was calculated in RAxML v. 8.2.11 (Stamatakis, 2014) (settings: *-f a* [rapid bootstrap analysis and search for best-scoring ML tree in one program run], *-m PROTGAMMAAUTO* [automatic protein substitution model selection with and without empirical base frequencies], *-N 100* [100 rapid bootstraps]). The tree was rooted by running RAxML with setting "if I" which simply balances subtree lengths. InterProScan (<https://www.ebi.ac.uk/interpro/>) was used for protein sequence analysis.

Signal peptides (if present) were determined with the SignalP v. 5.0 online tool (<http://www.cbs.dtu.dk/services/SignalP>) while

disulphide bonds were predicted using DISULFIND (<http://disulfind.dsi.unifi.it/>).

The detection of selective sweeps was conducted using a population genomics data set of 89 DMI-resistant *C. beticola* isolates collected in sugar beet fields near Fargo, North Dakota in 2016 (Spanner et al., unpublished data). The selective sweep analysis used OmegaPlus v. 3.0.3 (Alachiotis et al., 2012) and RAiSD v. 2.9. These methods detect outlier regions based on two statistics,  $\omega$  (OmegaPlus) and  $\mu$  (RAiSD) (Alachiotis & Pavlidis, 2018; Alachiotis et al., 2012; Excoffier et al., 2013). To control for the effect of demographic history of the population on the site frequency spectrum, linkage disequilibrium, and genetic diversity along the genome when setting the significance threshold (Nielsen et al., 2005; Pavlidis et al., 2013), we simulated data sets using the ms coalescent simulator (Hudson, 2002) under the best neutral demographic model, as inferred with fastsimcoal2 (Excoffier et al., 2013).

#### 4.7 | Protein structure prediction

Mature protein sequences were submitted to the I-TASSER online server for protein structure and function prediction (Roy et al., 2010; Yang et al., 2015; Zhang, 2008.). The query sequence was initially threaded through a nonredundant structure library (protein data bank, PDB) to identify structural templates, which were then used in an iterative Monte Carlo process to simulate protein structure. COACH analysis provided functional insight on ligand binding sites (LBS), Enzyme Commission (EC), and Gene Ontology (GO).

#### 4.8 | Quantitative reverse transcription PCR of *CbNip1*

Quantitative reverse transcription PCR (RT-qPCR) was performed in triplicate using the SensiMix SYBR Hi-Rox kit (BioLine) with an ABI 7300 PCR machine (Applied Biosystems) with cDNA of each time point for gene expression analysis and using the GoTaq qPCR Master Mix (Promega) with a CFX96 Real-Time System (Bio-Rad) with gDNA of each treatment for fungal biomass quantification. All reactions were done in triplicate and primers are listed in Table S4. Real-time PCR conditions started with a denaturation step of 10 min at 95 °C; followed by denaturation for 15 s at 95 °C, annealing for 30 s at 60 °C, and extension for 30 s at 72 °C, for 30 cycles. Water as template control was included for all qPCR runs. With *C. beticola actin* as a reference gene for the gene expression study, relative gene expression of three biological repetitions was calculated in comparison to the earliest measured time point using the Pfaffl method (Pfaffl, 2001). Variation in gene expression was calculated using the standard error of the means of three biological replicates. A one-way analysis of variance (ANOVA) ( $p < .05$ ) with a post hoc Tukey test using GNU SPSS (2015) was performed to determine statistical differences in gene expression level means between time points and subsequently determine differences by pairwise comparing

gene expression levels of different time points. Biomass was determined by quantifying the expression with SbEc1-F/SbEc1-R primers (De Coninck et al., 2012) for sugar beet (Table S4) and CbActin Fp/CbActin Rp primer for *C. beticola* (Table S4) and using the  $\Delta\Delta C_t$  method (Livak & Schmittgen, 2001) relative to the average value of the wild-type inoculated sugar beet plants. Error bars indicate standard error of variation between three individual biological replicates.

#### 4.9 | Vector construction and protein production in *E. coli*

For heterologous protein expression in *E. coli*, the *CbNip1* and *CB0940\_10646* coding sequence was amplified with GoTaq Long PCR Master Mix (Promega) from *C. beticola* 09-40 wild-type cDNA using primers MKE-78/77 and MKE-76/79 (Table S4), respectively. Amplicons and pET SUMO vector (Invitrogen) were digested with *EcoRI* and *NotI* and followed by ligation of the fragments into the double-digested pET SUMO vector with T4 DNA ligase (NEB) and cloned into *E. coli* DH5 $\alpha$ . Plasmids carrying the correct *CbNip1* or *CB0940\_10646* coding sequence were verified by sequencing (Eurofins Genomics, Ebersberg, Germany) as well as an empty pET SUMO vector subsequently cloned into the *E. coli* Origami (DE3) strain.

For heterologous protein expression, 1 L of Luria-Bertani (LB) broth was inoculated with 20 ml of a culture that was grown overnight in LB plus kanamycin 50  $\mu\text{g/ml}$  with either *CbNip1* pET expression construct or the empty vector control and grown at 37 °C, shaking at 200 rpm until an OD<sub>600</sub> of 0.6–0.8 was reached. Protein production was induced with 0.05 mM isopropyl  $\beta$ -D-1-thiogalactopyranoside (IPTG) final concentration and kept growing at 20 °C and shaking at 200 rpm for 24 hr. Cells were pelleted, snap frozen with liquid nitrogen and then lysed with 20 ml of lysis buffer containing 50 mM Tris.HCl pH 8.5 (Invitrogen) and 150 mM NaCl (Sigma), 10% glycerol (Amresco), 6 mg/ml lysozyme from chicken egg white (Sigma), 2 mg/ml sodium deoxycholate (Sigma), 0.625 mg/ml deoxyribonuclease I from bovine pancreas (Sigma), and one cOmplete protease inhibitor pill (Sigma). After the cultures were kept on ice for 1.5 hr, cells debris was spun down for 1 hr at 20,000  $\times g$  at 4 °C and the soluble protein fraction was processed for protein purification.

#### 4.10 | Protein purification

In *E. coli* heterologously produced protein samples were loaded at 1 ml/min onto a column packed with 2 ml of Ni Superflow resin (Clontech) for purification. After a washing step with wash buffer (50 mM Na<sub>2</sub>HPO<sub>4</sub>, 300 mM NaCl, 40 mM imidazole [Merck]) at 2 ml/min to wash out contaminative *E. coli* native proteins, small ubiquitin-like modifier (SUMO)-tagged *CbNip1* or the SUMO tag alone obtained from the empty vector sample were eluted with elution buffer (50 mM Na<sub>2</sub>HPO<sub>4</sub>, 300 mM NaCl, 250 mM imidazole). Elution samples were dialysed with a Spectra/Por dialysis membrane with

molecular weight cut-off (MWCO) of 3,500 (Spectrum Laboratories) against 200 mM NaCl containing ULP-1 enzyme to cleave off the SUMO tag at 4 °C overnight without agitation. The next day samples were run through the nickle bead column with the same setup as before at 1 ml/min to allow cleaved off SUMO tags to bind to the nickel beads. Flow-through was collected and again dialysed for 24 hr against 200 mM NaCl. Samples were concentrated with Amicon Ultra-15 centrifugal filter unit with an Ultracel-3 membrane (Millipore) with a 3 kDa cut-off. For visualization, 5  $\mu\text{l}$  of protein sample were loaded on Mini-PROTEAN TGX stain-free precast gels (Bio-Rad).

#### 4.11 | Refolding and preparation of CB0940\_10646 for sugar beet leaf infiltration

Synthesized mature CB0940\_10646 purchased from GeneScript was dissolved in Milli-Q water to 3 mg/ml. For refolding, oxidized glutathione (Sigma) and reduced glutathione (Sigma) were added to 1 mg/ml CB0940\_10646 to an end ratio of 5:1 mM and incubated overnight. Milli-Q water treated with the same glutathione ratio served as a control. To see whether the addition of trace elements leads to activation of necrosis-inducing activity of CB0940\_10646, 1  $\mu\text{l}$  of trace element stock was added to 0.5 ml of protein sample or water control to a trace element end concentration as found in Fries medium used for the culture filtrate experiment.

#### 4.12 | Protein infiltration

Sugar beet plants of the variety C093 were grown in the climate chamber at 21 °C with 10 hr light with 10 lux and 70% humidity. After 7 weeks approximately 30–50  $\mu\text{l}$  of purified protein (c.2 mg/ml) or empty vector (Figure S12) was infiltrated into the leaves using a 1 ml needleless syringe and the infiltration area was marked with a marker pen. Dark-treated leaves were wrapped in aluminium foil to prevent light exposure. For this experiment, CB0940\_10646 and three individually produced and purified *CbNip1* samples were infiltrated at least three times.

#### 4.13 | *CbNip1* deletion and ectopic mutants

Individual *CbNip1* deletion mutants were generated following the split-marker polyethylene glycol-protocol described in Bolton et al. (2016). Primers are listed in Table S4. Three individual *C. beticola* 09-40 *CbNip1* deletion mutants were confirmed by full genome sequencing using Oxford Nanopore MinION technology with the Rapid Sequencing Kit (Oxford Nanopore Technologies) to determine a single hygromycin B phosphotransferase insertion replaced the *CB0940\_03921* gene as shown in Figure S9. The ectopic mutant was confirmed by PCR by absence of amplicon for site-directed hygromycin integration, and presence of amplicons for hygromycin and *CbNip1* gene amplification (Figure S10).

#### 4.14 | *C. beticola* in vitro fitness assay

A 5 mm plug was taken from the actively growing zone of 4-day-old cultures of the wild type and three individual  $\Delta CbNip1$  mutants and used to inoculate PDA plates supplemented with sorbitol (1 M), Calcofluor (100  $\mu\text{g/ml}$ ), charcoal (0.01 g/ml), Congo red (45  $\mu\text{g/ml}$ ),  $\text{H}_2\text{O}_2$  (1 mM), or NaCl (1 M). Plates were incubated for 7 days at room temperature to observe fungal fitness and to take photographs.

#### 4.15 | Inoculation assay

Spore formation of *C. beticola* wild type, three individual  $\Delta CbNip1$  mutants, and one ectopic transformant was induced on CV8 agar plates as previously described (Secor & Rivera, 2012). Spores were harvested and adjusted to a concentration of  $10^5$  spores/ml and spore suspension was equally sprayed on the leaves of 5-week-old and 7-week-old sugar beet plants of the variety C093 for fungal biomass analysis and gene expression analysis, respectively. Inoculated plants were kept in a humidity chamber with about 27 °C and 90% humidity for 5 days after which plants were exposed to 22 °C with a 16-hr/8-hr day/night cycle. For fungal biomass analysis three leaves of three plants for three repetitions were harvested at 21 DPI<sub>noc</sub> and instantly snap frozen while plants for gene expression analysis were harvested at 3, 6, 9, 12, 15, 18, and 21 DPI<sub>noc</sub> using three leaves of two plants in three repetitions.






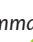

#### ACKNOWLEDGMENTS

M.D.B. is supported by USDA-ARS CRIS project 3060-22000-044 and grants from Beet Sugar Development Foundation and the Sugar Beet Research and Education Board of MN and ND. M.K.E. was supported by NWO grant 833.13.007.

#### DATA AVAILABILITY STATEMENT

The data that support the findings of this study are available from the corresponding author upon reasonable request.

#### ORCID

Malaika K. Ebert  <https://orcid.org/0000-0002-1891-6063>  
 Lorena I. Rangel  <https://orcid.org/0000-0002-9081-5275>  
 Rebecca E. Spanner  <https://orcid.org/0000-0002-4735-9649>  
 Timothy L. Friesen  <https://orcid.org/0000-0001-5634-2200>  
 Ronnie de Jonge  <https://orcid.org/0000-0001-5065-8538>  
 Gary A. Secor  <https://orcid.org/0000-0002-9908-7075>  
 Bart P. H. J. Thomma  <https://orcid.org/0000-0003-4125-4181>  
 Eva H. Stukenbrock  <https://orcid.org/0000-0001-8590-3345>  
 Melvin D. Bolton  <https://orcid.org/0000-0003-1197-2078>

#### REFERENCES

- Alachiotis, N. & Pavlidis, P. (2018) RAiSD detects positive selection based on multiple signatures of a selective sweep and SNP vectors. *Communications Biology*, 1, 79.
- Alachiotis, N., Stamatakis, A. & Pavlidis, P. (2012) OmegaPlus: a scalable tool for rapid detection of selective sweeps in whole-genome datasets. *Bioinformatics*, 28, 2274–2275.
- Allen, A., Chatt, E. & Smith, T.J. (2013) The Atomic structure of the virally encoded antifungal protein, KP6. *Journal of Molecular Biology*, 425, 609–621.
- Bailey, B.A. (1995) Purification of a protein from culture filtrates of *Fusarium oxysporum* that induces ethylene and necrosis in leaves of *Erythroxylum coca*. *Phytopathology*, 85, 1250–1255.
- Bailey, B.A., Dean, J.F.D. & Anderson, J.D. (1990) An ethylene biosynthesis-inducing endoxylanase elicits electrolyte leakage and necrosis in *Nicotiana tabacum* cv. Xanthi leaves. *Plant Physiology*, 94, 1849–1854.
- Ben M'Barek, S., Cordewener, J.H., Tabib Ghaffary, S.M., van der Lee, T.A., Liu, Z., Mirzadi Gohari, A. et al. (2015) FPLC and liquid-chromatography mass spectrometry identify candidate necrosis-inducing proteins from culture filtrates of the fungal wheat pathogen *Zymoseptoria tritici*. *Fungal Genetics and Biology*, 79, 54–62.
- Bird, L.J., Coleman, M.L. & Newman, D.K. (2013) Iron and copper act synergistically to delay anaerobic growth of bacteria. *Applied and Environmental Microbiology*, 79, 3619–3627.
- Bolton, M.D., Ebert, M.K., Faino, L., Rivera-Varas, V., de Jonge, R., Van de Peer, Y. et al. (2016) RNA-sequencing of *Cercospora beticola* DMI-sensitive and -resistant isolates after treatment with tetraconazole identifies common and contrasting pathway induction. *Fungal Genetics and Biology*, 92, 1–13.
- Bolton, M.D., Secor, G.A., Rivera, V., Weiland, J.J., Rudolph, K., Birla, K. et al. (2012) Evaluation of the potential for sexual reproduction in field populations of *Cercospora beticola* from USA. *Fungal Biology*, 116, 511–521.
- Brito, N., Espino, J.J. & González, C. (2006) The endo- $\beta$ -1,4-xylanase xyn11A is required for virulence in *Botrytis cinerea*. *Molecular Plant-Microbe Interactions*, 19, 25–32.
- Callahan, T.M., Rose, M.S., Meade, M.J., Ehrenshaft, M. & Upchurch, R.G. (1999) CFP, the putative cercosporin transporter of *Cercospora kikuchii*, is required for wild type cercosporin production, resistance, and virulence on soybean. *Molecular Plant-Microbe Interactions*, 12, 901–910.
- Capella-Gutiérrez, S., Silla-Martínez, J.M. & Gabaldón, T. (2009) trimAl: a tool for automated alignment trimming in large-scale phylogenetic analyses. *Bioinformatics*, 25, 1972–1973.
- Changela, A., Chen, K., Xue, Y., Holschen, J., Outten, C.E., O'Halloran, T.V. et al. (2003) Molecular basis of metal-ion selectivity and zeptomolar sensitivity by CueR. *Science*, 301, 1383–1387.
- Choquer, M., Dekkers, K.L., Chen, H.-Q., Cao, L., Ueng, P.P., Daub, M.E. et al. (2005) The CTB1 gene encoding a fungal polyketide synthase is required for cercosporin biosynthesis and fungal virulence of *Cercospora nicotianae*. *Molecular Plant-Microbe Interactions*, 18, 468–476.
- Daub, M.E. & Ehrenshaft, M. (2000) The photoactivated *Cercospora* toxin cercosporin: contributions to plant disease and fundamental biology. *Annual Review of Phytopathology*, 38, 461–490.
- De Coninck, B.M.A., Amand, O., Delauré, S.L., Lucas, S., Hias, N., Weyens, G. et al. (2012) The use of digital image analysis and real-time PCR fine-tunes bioassays for quantification of cercospora leaf spot disease in sugar beet breeding. *Plant Pathology*, 61, 76–84.
- Excoffier, L., Dupanloup, I., Huerta-Sánchez, E., Sousa, V.C. & Foll, M. (2013) Robust demographic inference from genomic and SNP data. *PLoS Genetics*, 9, e1003905.
- Faris, J.D., Zhang, Z., Lu, H., Lu, S., Reddy, L., Cloutier, S. et al. (2010) A unique wheat disease resistance-like gene governs effector-triggered susceptibility to necrotrophic pathogens. *Proceedings of the National Academy of Sciences of the United States of America*, 107, 13544–13549.
- Feindt, F., Mendgen, K. & Heitefuss, R. (1981) Feinstruktur unterschiedlicher Zellwandreaktionen im Blattparenchym anfälliger und

- resistenter Rüben (*Beta vulgaris* L.) nach Infektion durch *Cercospora beticola* Sacc. *Journal of Phytopathology*, 101, 248–264.
- Fellbrich, G., Romanski, A., Varet, A., Blume, B., Brunner, F., Engelhardt, S. et al. (2002) NPP1, a *Phytophthora*-associated trigger of plant defense in parsley and *Arabidopsis*. *The Plant Journal*, 32, 375–390.
- Finkler, A., Peery, T., Tao, J., Bruenn, J. & Koltin, I. (1992) Immunity and resistance to the KP6 toxin of *Ustilago maydis*. *Molecular and General Genetics*, 233, 395–403.
- Flor, H.H. (1942) Inheritance of pathogenicity in *Melampsora lini*. *Phytopathology*, 32, 653–669.
- Friesen, T.L. & Faris, J.D. (2012) Characterization of plant–fungal interactions involving necrotrophic effector-producing plant pathogens. In: Bolton, M.D. and Thomma, B.P.H.J. (Eds.) *Plant fungal pathogens: methods and protocols*. Totowa, NJ: Humana Press, pp. 191–207.
- Friesen, T.L., Faris, J.D., Solomon, P.S. & Oliver, R.P. (2008) Host-specific toxins: effectors of necrotrophic pathogenicity. *Cellular Microbiology*, 10, 1421–1428.
- Friesen, T.L., Meinhardt, S.W. & Faris, J.D. (2007) The *Stagonospora nodorum*–wheat pathosystem involves multiple proteinaceous host-selective toxins and corresponding host sensitivity genes that interact in an inverse gene-for-gene manner. *The Plant Journal*, 51, 681–692.
- Fulton T.M., Chunwongse J., Tanksley S.D. (1995) Microprep protocol for extraction of DNA from tomato and other herbaceous plants. *Plant Molecular Biology Reporter*, 13, 207–209.
- Gijzen, M. & Nürnberger, T. (2006) Nep1-like proteins from plant pathogens: Recruitment and diversification of the NPP1 domain across taxa. *Phytochemistry*, 67, 1800–1807.
- GNU Project (2015) *GNU PSPP for GNU/Linux* (Version 0.8.5) [Computer Software]. Boston, MA: Free Software Foundation. Available from: <https://www.gnu.org/software/pspp/> [Accessed 24 July 2020].
- Guo, A., Reimers, P.J. & Leach, J.E. (1993) Effect of light on incompatible interactions between *Xanthomonas oryzae* pv. *oryzae* and rice. *Physiological and Molecular Plant Pathology*, 42, 413–425.
- Horbach, R., Navarro-Quesada, A.R., Knogge, W. & Deising, H.B. (2011) When and how to kill a plant cell: infection strategies of plant pathogenic fungi. *Journal of Plant Physiology*, 168, 51–62.
- Hudson R.R. (2002) Generating samples under a Wright-Fisher neutral model of genetic variation. *Bioinformatics*, 18, 337–338.
- Inohara, N. & Nuñez, G. (2002) ML–A conserved domain involved in innate immunity and lipid metabolism. *Trends in Biochemical Sciences*, 27, 219–221.
- Jalal, M.A.F., Hossain, M.B., Robeson, D.J. & van der Helm, D. (1992) *Cercospora beticola* phytotoxins: cebetins that are photoactive, magnesium ion-binding, chlorinated anthraquinone–xanthone conjugates. *Journal of the American Chemical Society*, 114, 5967–5971.
- de Jonge, R., Ebert, M.K., Huitt-Roehl, C.R., Pal, P., Suttle, J.C., Spanner, R.E. et al. (2018) Gene cluster conservation provides insight into cercosporin biosynthesis and extends production to the genus *Colletotrichum*. *Proceedings of the National Academy of Sciences of the United States of America*, 115, E5459–E5466.
- Kairys, V., Gilson, M.K. & Luy, B. (2004) Structural model for an AxxxG-mediated dimer of surfactant-associated protein C. *European Journal of Biochemistry*, 271, 2086–2092.
- Kami, C., Lorrain, S., Hornitschek, P. & Fankhauser, C. (2010) Light-regulated plant growth and development. *Current Topics in Developmental Biology*, 91, 29–66.
- Kars, I., Krooshof, G.H., Wagemakers, L., Joosten, R., Benen, J.A.E. & Kan, J.A.L.V. (2005) Necrotizing activity of five *Botrytis cinerea* endopolygalacturonases produced in *Pichia pastoris*. *The Plant Journal*, 43, 213–225.
- Katoh, K. & Standley, D.M. (2013) MAFFT multiple sequence alignment software version 7: improvements in performance and usability. *Molecular Biology and Evolution*, 30, 772–780.
- Kettles, G.J., Bayon, C., Canning, G., Rudd, J.J. & Kanyuka, K. (2017) Apoplastic recognition of multiple candidate effectors from the wheat pathogen *Zymoseptoria tritici* in the nonhost plant *Nicotiana benthamiana*. *New Phytologist*, 213, 338–350.
- Kettles, G.J., Bayon, C., Sparks, C.A., Canning, G., Kanyuka, K. & Rudd, J.J. (2018) Characterization of an antimicrobial and phytotoxic ribonuclease secreted by the fungal wheat pathogen *Zymoseptoria tritici*. *New Phytologist*, 217, 320–331.
- Khan, M.F.R. & Khan, J. (2010) Survival, spore trapping, dispersal, and primary infection site for *Cercospora beticola* in sugar beet. In: Lartey, R.T., Weiland, J.J., Panella, L., Crous, P.W. & Windels, C.E. (Eds.) *Cercospora leaf spot of sugar beet and related species*. St Paul, MN: APS Press, pp. 67–75.
- Kim, H., Ridenour, J.B., Dunkle, L.D. & Bluhm, B.H. (2011) Regulation of stomatal tropism and infection by light in *Cercospora zeae-maydis*: evidence for coordinated host/pathogen responses to photoperiod? *PLoS Pathogens*, 7, e1002113.
- Koltin, Y. & Day, P. (1975) Specificity of *Ustilago maydis* killer proteins. *Applied Microbiology*, 30, 694–696.
- Laugé, R., Joosten, M.H.A.J., Haanstra, J.P.W., Goodwin, P.H., Lindhout, P. & De Wit, P.J.G.M. (1998) Successful search for a resistance gene in tomato targeted against a virulence factor of a fungal pathogen. *Proceedings of the National Academy of Sciences of the United States of America*, 95, 9014–9018.
- Liu, Z., Faris, J., Meinhardt, S., Ali, S., Rasmussen, J. & Friesen, T. (2004) Genetic and physical mapping of a gene conditioning sensitivity in wheat to a partially purified host-selective toxin produced by *Stagonospora nodorum*. *Phytopathology*, 94, 1056–1060.
- Liu, Z., Faris, J.D., Oliver, R.P., Tan, K.-C., Solomon, P.S., McDonald, M.C. et al. (2009) SnTox3 acts in effector triggered susceptibility to induce disease on wheat carrying the *Snn3* gene. *PLoS Pathogens*, 5, e1000581.
- Liu, Z., Zhang, Z., Faris, J.D., Oliver, R.P., Syme, R., McDonald, M.C. et al. (2012) The cysteine rich necrotrophic effector SnTox1 produced by *Stagonospora nodorum* triggers susceptibility of wheat lines harboring *Snn1*. *PLoS Pathogens*, 8, e1002467.
- Livak, K.J. & Schmittgen, T.D. (2001) Analysis of relative gene expression data using real-time quantitative PCR and the  $2^{-\Delta\Delta Ct}$  method. *Methods*, 25, 402–408.
- Motteram, J., Kufner, I., Deller, S., Brunner, F., Hammond-Kosack, K.E., Nürnberger, T. et al. (2009) Molecular characterization and functional analysis of MgNLP, the sole NPP1 domain-containing protein, from the fungal wheat leaf pathogen *Mycosphaerella graminicola*. *Molecular Plant-Microbe Interactions*, 22, 790–799.
- Mullen, G.E.D., Kennedy, M.N., Visintin, A., Mazzoni, A., Leifer, C.A., Davies, D.R. et al. (2003) The role of disulfide bonds in the assembly and function of MD-2. *Proceedings of the National Academy of Sciences of the United States of America*, 100, 3919–3924.
- Nielsen R., Williamson, S., Kim, Y., Hubisz, M.J., Clark, A.G. & Bustamante, C. (2005) Genomic scans for selective sweeps using SNP data. *Genome Research*, 15, 1566–1575.
- Pavlidis P., Živković D., Stamatakis A., Alachiotis N. (2013) SweeD: Likelihood-based detection of selective sweeps in thousands of genomes. *Molecular Biology and Evolution*, 30, 2224–2234.
- Pemberton, C.L. & Salmond, G.P.C. (2004) The Nep1-like proteins – a growing family of microbial elicitors of plant necrosis. *Molecular Plant Pathology*, 5, 353–359.
- Pfaffl, M.W. (2001) A new mathematical model for relative quantification in real-time RT-PCR. *Nucleic Acids Research*, 29, e45.
- Qi, T., Seong, K., Thomazella, D.P.T., Kim, J.R., Pham, J., Seo, E. et al. (2018) NRG1 functions downstream of EDS1 to regulate TIR-NLR-mediated plant immunity in *Nicotiana benthamiana*. *Proceedings of the National Academy of Sciences of the United States of America*, 115, E10979–E10987.

- Raffaello, T. & Asiegbu, F.O. (2017) Small secreted proteins from the necrotrophic conifer pathogen *Heterobasidion annosum* s.l. (HaSSPs) induce cell death in *Nicotiana benthamiana*. *Scientific Reports*, 7, 8000.
- Rangel, L.I., Spanner, R.E., Ebert, M.K., Pethybridge, S.J., Stukenbrock, E.H., de Jonge, R. et al. (2020) *Cercospora beticola*: The intoxicating lifestyle of the leaf spot pathogen of sugar beet. *Molecular Plant Pathology*, 21, 1020–1041.
- Rathaiah, Y. (1977) Stomatal tropism of *Cercospora beticola* in sugarbeet. *Phytopathology*, 67, 358–362.
- Roberts, M.R. & Paul, N.D. (2006) Seduced by the dark side: integrating molecular and ecological perspectives on the influence of light on plant defence against pests and pathogens. *New Phytologist*, 170, 677–699.
- Roden, L.C. & Ingle, R.A. (2009) Lights, rhythms, infection: the role of light and the circadian clock in determining the outcome of plant-pathogen interactions. *The Plant Cell*, 21, 2546–2552.
- Roy, A., Kucukural, A. & Zhang, Y. (2010) I-TASSER: a unified platform for automated protein structure and function prediction. *Nature Protocols*, 5, 725–738.
- Schlösser, E. (1962) Über eine biologisch aktive Substanz aus *Cercospora beticola*. *Journal of Phytopathology*, 44, 295–312.
- Secor, G.A. & Rivera, V.V. (2012) Fungicide resistance assays for fungal plant pathogens. *Plant Fungal Pathogens: Methods and Protocols*, 385–392.
- Shi, G., Zhang, Z., Friesen, T.L., Raats, D., Fahima, T., Brueggeman, R.S. et al. (2016) The hijacking of a receptor kinase-driven pathway by a wheat fungal pathogen leads to disease. *Science Advances*, 2, e1600822.
- Smith, J.M. & Haigh, J. (1974) The hitch-hiking effect of a favourable gene. *Genetics Research*, 23, 23–35.
- Solel, Z. & Minz, G. (1971) Infection process of *Cercospora beticola* in sugarbeet in relation to susceptibility. *Phytopathology*, 61, 463–466.
- Sperschneider, J., Dodds, P.N., Gardiner, D.M., Singh, K.B. & Taylor, J.M. (2018) Improved prediction of fungal effector proteins from secretomes with EffectorP 2.0. *Molecular Plant Pathology*, 19, 2094–2110.
- Stamatakis, A. (2014) RAxML version 8: a tool for phylogenetic analysis and post-analysis of large phylogenies. *Bioinformatics*, 30, 1312–1313.
- Steinkamp, M.P., Martin, S.S., Hoefert, L.L. & Ruppel, E.G. (1979) Ultrastructure of lesions produced by *Cercospora beticola* in leaves of *Beta vulgaris*. *Physiological Plant Pathology*, 15, 13–26.
- Thomma, B.P.H.J., Seidl, M.F., Shi-Kunne, X., Cook, D.E., Bolton, M.D., van Kan, J.A.L. et al. (2016) Mind the gap; seven reasons to close fragmented genome assemblies. *Fungal Genetics and Biology*, 90, 24–30.
- Weltmeier, F., Mäser, A., Menze, A., Hennig, S., Schad, M., Breuer, F. et al. (2011) Transcript profiles in sugar beet genotypes uncover timing and strength of defense reactions to *Cercospora beticola* infection. *Molecular Plant-Microbe Interactions*, 24, 758–772.
- Yamazaki, S., Okubo, A., Akiyama, Y. & Fuwa, K. (1975) Cercosporin, a novel photodynamic pigment isolated from *Cercospora kikuchii*. *Agricultural and Biological Chemistry*, 39, 287–288.
- Yang, J., Yan, R., Roy, A., Xu, D., Poisson, J. & Zhang, Y. (2015) The I-TASSER suite: protein structure and function prediction. *Nature Methods*, 12, 7–8.
- Zhang, Y. (2008) I-TASSER server for protein 3D structure prediction. *BMC Bioinformatics*, 9, 40.

## SUPPORTING INFORMATION

Additional Supporting Information may be found online in the Supporting Information section.

**How to cite this article:** Ebert MK, Rangel LI, Spanner RE, et al. Identification and characterization of *Cercospora beticola* necrosis-inducing effector CbNip1. *Mol Plant Pathol.* 2020;00:1–16. <https://doi.org/10.1111/mpp.13026>